Opto-Electronic Advances

Review

2022, Vol. 5, No. 6

DOI: 10.29026/oea.2022.210174

Nonlinear optics with structured light

Wagner Tavares Buono* and Andrew Forbes*

The interest in tailoring light in all its degrees of freedom is steadily gaining traction, driven by the tremendous developments in the toolkit for the creation, control and detection of what is now called structured light. Because the complexity of these optical fields is generally understood in terms of interference, the tools have historically been linear optical elements that create the desired superpositions. For this reason, despite the long and impressive history of nonlinear optics, only recently has the spatial structure of light in nonlinear processes come to the fore. In this review we provide a concise theoretical framework for understanding nonlinear optics in the context of structured light, offering an overview and perspective on the progress made, and the challenges that remain.

Keywords: wave mixing; parametric conversion; high harmonic generation; structured light; photonic crystals; holography; nonlinear optics; second harmonic generation; metasurfaces

Buono WT, Forbes A. Nonlinear optics with structured light. *Opto-Electron Adv* **5**, 210174 (2022).

Introduction

Structured light[1] refers to the modern-day ability to tailor light in all its degrees of freedom (DoFs), spatial and temporal, to create complex optical fields in both the classical[2–5] and quantum[6,7] domains. Combining DoFs have given rise to novel and exotic states of light as 2D, 3D and even 4D fields, including optical knots[8,9], skyrmions[10,11], Mobius strips[12], spatio-temporal fields[13–16], ray-wave structured fields[17,18], quantum-like classical light[19–21] and photonic wheels[22]. But although the progress has been rapid of late, the topic itself can be dated back to Thomas Young and his double slit experiment, where arguably the first structured light was created. Indeed, the very essence of structured light is the notion of superpositions, where interference (not necessarily in intensity) gives rise to the desired structure. Today one can formulate all of structured light as a linear superposition principle[1], giving rise to geometric representations of the superpositions, from the orbital angular momentum (OAM)[23], to the total angular momentum[24] of light, and more recently a generalised framework for multiple DoFs[25]. For example, even simple plane waves hold the potential for structure: one plane wave may have a phase gradient, two plane waves will give rise to an intensity structure (as done by Young more than 200 years ago), three plane waves can produce an optical phase singularity, while multiple plane waves can give rise to exotic families of structured light, for instance, planes waves travelling on a cone give rise to Bessel beams[26]. If the interfering plane waves are allowed to hold information in another DoF, say polarization, then just two can create exotic polarization structures[27] and if focussed, will create synthetic chiral light in 3D[28]. It is clear that there is a strong link between interference, a linear effect, and structured light. For this reason, the vast bulk of studies involving structured light have considered linear optical elements, with only much more recent progress in nonlinear optics with structured light, the topic of this review.

The invention of the laser[29] is seen as fundamental to the development of the research field of nonlinear optics,

School of Physics, University of the Witwatersrand, Private Bag 3, Johannesburg 2050, South Africa.

*Correspondence: WT Buono, E-mail: wagner.tavaresbuono@wits.ac.za; A Forbes, E-mail: andrew.forbes@wits.ac.za

Received: 18 December 2021; Accepted: 14 April 2022; Published online: 22 June 2022

with the first nonlinear optical demonstration of second harmonic generation (SHG)[30] following quickly, soon after by third harmonic generation[31] and SHG carrying spin angular momentum (SAM)[32]. The reason for the strong historical linkage is simple: nonlinear optical phenomena are weak and typically need a coherent high power source to be observed. This knowledge can be dated back as far a Fresnel, who already understood that wave superpositions could transcend the linear regime. With the development of stronger laser sources and more efficient nonlinear materials, we have overcome this requirement. It is only natural then that the study of nonlinear optical phenomena shifts from asking "how much light is there?" based on efficiency concerns (intensity being the key to address this), to "what does the light look like?" (the structure of the light). Seminal works began analysing the structure of the generated light three decades ago[33] with early work demonstrating the doubling of the number of singularities in the generated field[34]. Following the link between orbital angular momentum (OAM) and these so-called screw dislocations (see ref.[35] and references therein), the use of OAM carrying Laguerre-Gaussian (LG) modes in nonlinear optics was demonstrated[36] followed a little later by the first production of quantum structured photons by nonlinear optics, demonstrating OAM entangled states[37]. Although these important works set the scene, further progress has been slow, until only recently.

In this review we follow the progress in the field, from intensity drive processes that serve to alter the frequency of the pump light, to the present day nonlinear toolkit for the creation, manipulation and detection of structured light. We begin with the familiar wave mixing processes of second order, which have been deeply explored and continue to develop to this day, serving to exemplify how counter-intuitive these interactions can be with the introduction of structured light. We then move on to show the types of media that allow these process and how they can also be structured, playing a crucial role in recent advances. We expand into higher-order parametric processes, including third harmonic generation and the generation of optical vortex solitons. Finally, we cite recent developments in high harmonic generation, an extreme non-parametric process, and the unusual applications of nonlinear processes in the quantum regime.

Theoretical background

The field of nonlinear optics is a venerable topic, and the reader is referred to excellent textbooks on the topic[38–40]. For the benefit of the reader, We begin by briefly outlining the core theory needed for the review, and to this end we begin with Maxwell's equations in the presence of a medium. If condensed and rewritten in terms of a wave equation, one finds,

$$\left[\nabla\times\nabla\times+\frac{1}{c^2}\frac{\partial^2}{\partial t^2}\right]\boldsymbol{E}=-\frac{4\pi}{c^2}\frac{\partial^2\boldsymbol{P}}{\partial t^2}\ , \tag{1}$$

where $\boldsymbol{E}$ is the electric field and $\boldsymbol{P}$ is the polarization of the medium. This describes the response of the medium to the input electric field, and the counter response of the polarised medium on the field. In a analogy to the harmonic oscillator, we can do a perturbative expansion of the medium polarization in a power series of the electric field strength,

$$P_i=\chi^{(1)}_{ij}E_j+\chi^{(2)}_{ijk}E_jE_k+\chi^{(3)}_{ijkl}E_jE_kE_l+\cdots\ , \tag{2}$$

where P_i is the i component of $\boldsymbol{P}$ and $\chi^{(n)}$ is the n−th order susceptibility tensor, a tensor of the n−th order. The first term is responsible for the well known linear optical effects, such as refraction and birefringence. All other terms are referred to as *nonlinear parametric effects*, which this review will mostly feature. This expansion describes a plethora of nonlinear optical effects, such as wave-mixing, self and cross phase modulation, among many. For example, the second order term, with its second order susceptibility tensor, allows the medium polarisability to be separated in frequency components. Second order wave mixing can result in effects such as second harmonic generation, sum frequency generation, difference frequency generation and optical rectification, with a well understood rule set.

But what are the governing principles when the light has internal structure? In this review we will often use scalar and vectorial combinations of light that carries OAM, a highly topical example. Such modes of light have an azimuthal phase profile given by $\exp(i\ell\phi)$, where ϕ is the azimuthal angle and ℓ is the topological charge, for photons with $\ell\hbar$ of OAM. For brievity we will refer to OAM modes by their topological charge, ℓ. What are the selection rules when such complex light fields are used in nonlinear processes? As we will show, the development of nonlinear optics with structure light has produced complex behaviour with some as yet unanswered questions. Further, it is not always possible to find exact solutions for the coupled equations that describe these phenomena. For instance, nonlinear processes of even the second order can generate coupled wave equations whose number increases directly with the number of transverse modes involved.

With suitable approximations (such as the slowly varying envelope approximation and lossless media) the generated field in three wave mixing can take the form

$$\frac{\partial E_3^{(\omega_3)}(\boldsymbol{r})}{\partial z} \propto \chi^{(2)} E_1^{(\omega_1)}(\boldsymbol{r}) E_2^{(\omega_2)}(\boldsymbol{r}) \,. \tag{3}$$

Similar differential equations are also derived for each frequency, initially obtaining three coupled differential equations. While these equations were initally derived as plane waves, structured light reveals more intricate interactions. For example, the phases and intensities are all intertwined: reshaping one field can mean completely new dynamics and new structures in all three involved fields. Due to the low conversion efficiency, a characteristic of nonlinear processes, in single-pass geometry we can make use of the non-depletion approximation, where the input fields can be regarded as static and therefore do not change on propagation. These equations show one remarkable feature of nonlinear optics: *the nontriviality of the superposition principle*. For example, let us associate the generated field $E_3'(\boldsymbol{r})$ with input fields $\{E_1'(\boldsymbol{r}), E_2'(\boldsymbol{r})\}$ and generated field $E_3''(\boldsymbol{r})$ with input fields $\{E_1''(\boldsymbol{r}), E_2''(\boldsymbol{r})\}$. If now we use as inputs $E_1(\boldsymbol{r}) = E_1'(\boldsymbol{r}) + E_2''(\boldsymbol{r})$ and $E_2(\boldsymbol{r}) = E_2'(\boldsymbol{r}) + E_2''(\boldsymbol{r})$ it will not follow that $E_3(\boldsymbol{r}) = E_3'(\boldsymbol{r}) + E_3''(\boldsymbol{r})$. In this equation, the vector nature of this interaction was omitted for simplicity, but it suffices to say that input fields have the same polarization for type-I and orthogonal polarizations for type-II. Equation (3) describes sum frequency generation (where $\omega_3 = \omega_2 + \omega_1$) and, if considered difference frequency generation ($\omega_3 = \omega_2 - \omega_1$), one of the fields ($\omega_1$) would be complex conjugated. For second harmonic generation both fundamental fields would have the same frequency ($\omega_3 = 2\omega_1 = 2\omega_2$) and the two fundamental fields would be identical for type-I but not necessarily for type-II.

The expansion of these fields into propagating waves in different directions gives us the phase-matching quantity

$$\Delta \boldsymbol{k} = \boldsymbol{k}_{\omega_3} \cdot \boldsymbol{r}_3 - \boldsymbol{k}_{\omega_1} \cdot \boldsymbol{r}_1 - \boldsymbol{k}_{\omega_2} \cdot \boldsymbol{r}_2 . \tag{4}$$

That ensures that the light generated is through a coherent process and interferes constructively at each wavefront generation. When $\Delta \boldsymbol{k} = 0$, this is referred to as perfect phase-matching.

Figure 1 highlights a few differences between the linear and nonlinear regimes, the latter illustrated using second harmonic generation as an example. We illustrate that the generated spatial structure is not simply a superposition, but the product of input modes. A consequence is that while the original modes may be

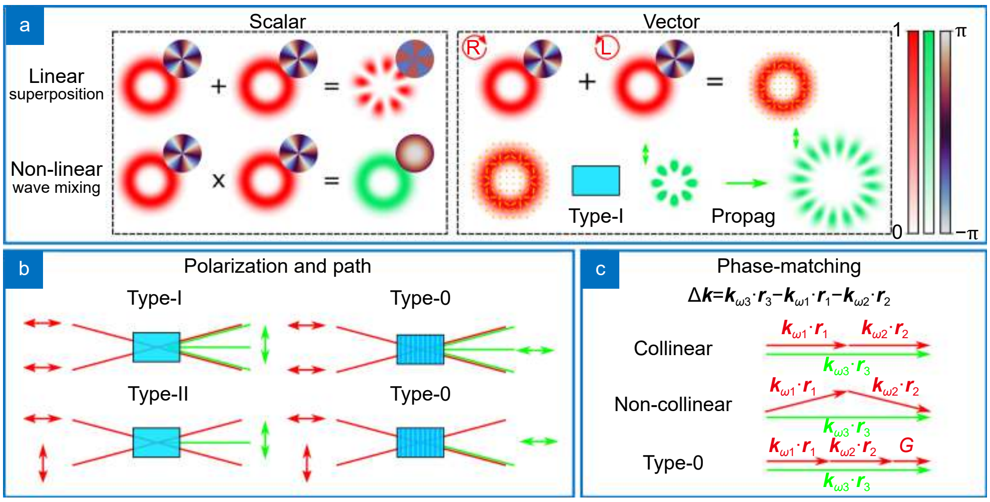

Fig. 1 | Linear and nonlinear processes. Using second harmonic generation (SHG), we illustrate the differences between linear and nonlinear processes. (**a**) Linear processes produce an output mode that is the addition of two input spatial modes of light, while SHG produces the product of the two modes. The linear superposition of two different modes with orthogonal polarization states generates a vector beam, which has a inhomogeneous polarization state. The polarization profile is represented as yellow lines across the transverse profile. In SHG, and wave mixing in general, the polarization profile will dictate where wave mixing happens and thus alter directly the spatial profile. In (**b**) we show exemplify how path can also be controlled via polarization and the different phase matching conditions of crystals, including the periodic poling of type-0. The mechanism which allows these interactions is sketched in (**c**). Phase-matching is the condition necessary for wave mixing to occur and exploits birefringence (types I and II) or periodical polling (type-0) to achieve it.

eigenmodes of free space, the final mode may not. For instance, as shown in Fig. 1(a), if two OAM modes with topological charges of $\ell = 4$ and $\ell = -4$ combine, then the superposition creates a petal-like structured which is stable in propagation, while the nonlinear process creates a ring-like structure with no OAM, which is unstable in propagation.

Polarization also has a non-immediate role. In the linear regime, optical beams with orthogonal polarization states do not interfere to produce fringes (but they do produce fringes in polarization[27,41]). In contrast, in nonlinear media, they do interact through the coupled interactions with the medium. If the input beam has a inhomogenous polarization profile, i.e. vector beam, then this interaction is different in every point of the transverse profile. We illustrate this in Fig. 1(b) where a vector beam used as input shows that SHG has different efficiencies across the transverse profile. This can be seen as a projection onto one of the crystals axis, generating a beam with a uniform polarization state and its spatial structure is influenced by both polarization and structures of the fundamental beams. This dependency creates states that binds path, input polarization and spatial mode. To understand the connection, one can consider the schematics in Fig. 1(b). The perfect phase-matching condition can be fulfilled for more than one propagation direction at the same time, each as independent processes. The wavevectors in this equation are considered inside the matter (often a crystal), where differently polarized beams would see different refractive indices, crafted specifically to fulfill this condition in types I and II. For type-0, the material is structured with a periodic polling, which gives a contribution of $G_m = m2\pi/\Lambda$ to phase-matching where Λ is the domain length.

The combination of Eqs. (3) and (4) exemplifies the role structured light's degrees of freedom (DoF) in wave mixing, encompassing spatial profiles through the coupled wave equations (Eq. (3)), polarization in the phase-matching (both in $\chi^{(2)}$ and $k_{x,y,z}$) and path in the phase-matching $\Delta\boldsymbol{k}$. Only by considering all these DoF and their interaction we can grasp a full understanding of nonlinear processes with structured light.

Structured dofs and their nonlinear coupling

By choosing sum-frequency generation and breaking wavelength degeneracy, it is possible to encode different structures in each frequency. If one of the fields is physically expanded and thus approximated to be a plane wave, we see the directly transfer and manipulation of the spatial profile of a beam across wavelengths[42–44]. In this case, the lack of structure of one field enables the generated beam to completely inherit the structure from the other. By using different spatial modes in each frequency, it was possible to perform OAM algebra[45]. This creates an interesting interaction where the wavelength is used as a control parameter for the spatial structure.

In initial works with SHG it was observed that the generated field would be proportional to the square of the fundamental frequency[36], as it is possible to see in Eq. (3) if the conditions $\omega_3 = 2\omega_2 = 2\omega_1$ and $E_1 = E_2$ are set. This describes type-I phase matching. If the vectorial nature of this interaction with matter is chosen accordingly, it is possible to use type-II phase matching to have different spatial modes in the same frequency but different polarizations[46,47], creating in the SHG a profile composed of the product of two different modes of the same frequency. Even in the collinear geometry configuration, there is an interplay between the spatial and polarization degrees of freedom.

The path degree of freedom can also be used: in Eq. (4) we can see that the phase-matching depends not only on the material but on the propagation direction of the beams. If two beams are crossed inside the crystal so that the phase-matching is fulfilled, a third beam is generated, as illustrated in Fig. 1(c). Using this it was possible to study the transverse structure transfer in SHG[48] and off axis singularity combination[49]. In these cases (the former is shown in Fig. 2(a)) one input wave can be approximated as a plane wave and the other has nonzero OAM. The non-collinear interaction generates the second harmonic of both input modes with the square of the spatial profile but also creates a third beam with the product of them, having the same OAM as the input, but different polarization and wavelength.

The three process depicted above are independent and do not interfere with each other. Interestingly, not all nonlinear process are independent. Using polarization as a control parameter in type-II SHG, the authors realized that nonlinear process can interfere destructively[50]. As illustrated in Fig. 2(b) two input beams with opposite OAM and orthogonal polarization states pass through a half-wave plate (HWP) at an angle θ and impinge at the crystal with a small angle. When $\theta = 0$ the phase matching conditions are only satisfied for one path. For $\theta = 22.5°$ all three paths have equal phase-matching

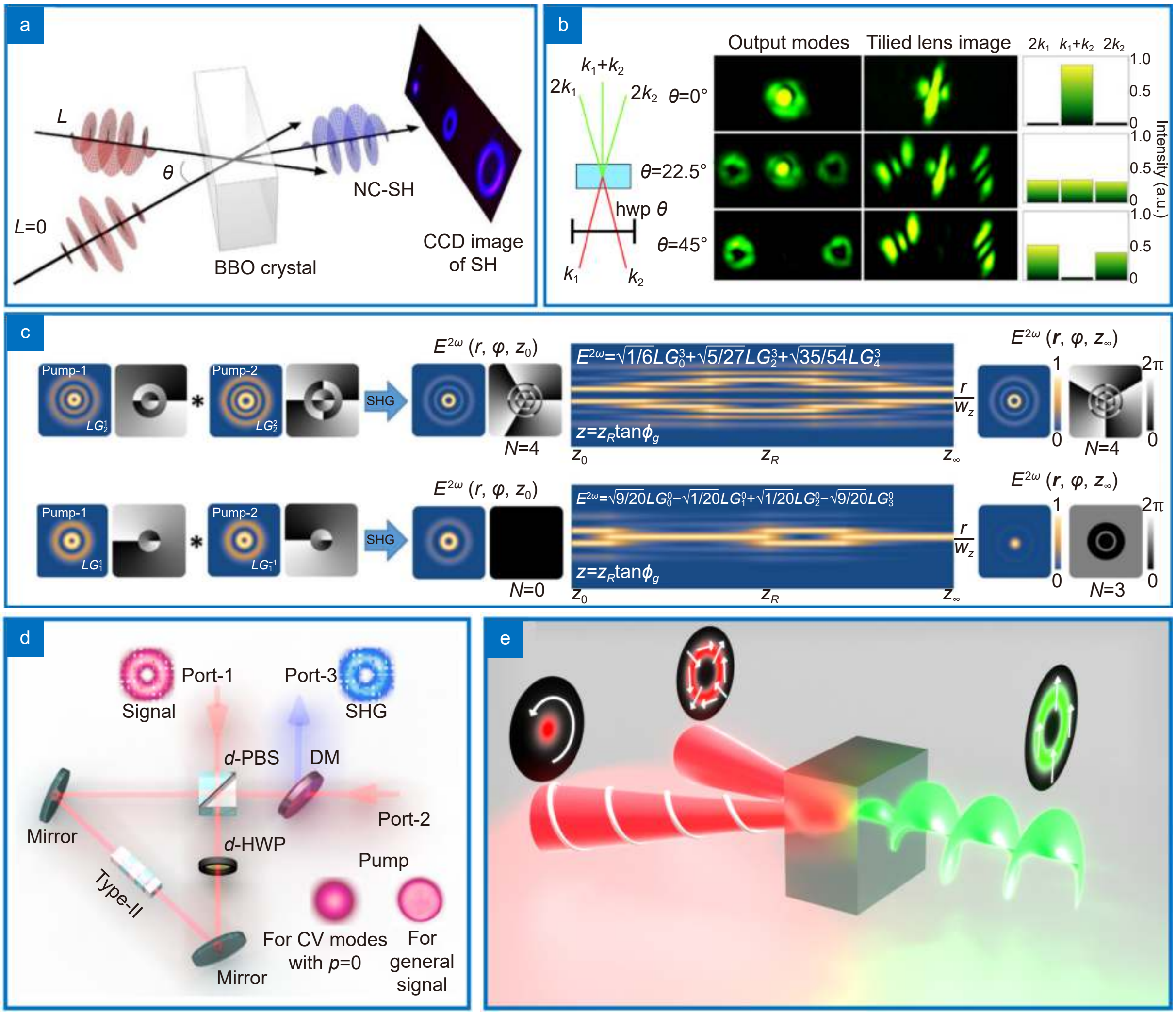

Fig. 2 | Wave mixing with different degrees of freedom. In (**a**), the authors show OAM algebra in noncollinear SHG. When type-II phase-matching is used, the same noncollinear geometry allows for polarization switching, shown in (**b**). This effectively couples multiple degrees of freedom in a single process: path, polarization, radial and angular transverse structures. The radial selection rules of LG modes in wave mixing are demonstrated in (**c**). There is a intrinsic relation between the radial and angular degrees of freedom, which is manifested in the propagation dependence of the spatial profiles. In (**d**), a experimental scheme using a Sagnac interferometer achieves faithful frequency conversion of vector light. Spin and orbital angular momentum are combined in second harmonic generation in (**e**). Figure repoduced with permission from: (a) ref.[48], Springer Nature; (b) ref.[50], © Optica Publishing Group; (c) ref.[54], © American Physical Society; (d) ref.[69], American Physical Society; (e) ref.[70], under aCreative Commons Attribution 4.0 International License

conditions satisfied and therefore equal intensities. However, when $\theta = 45°$ the phase matching conditions are satisfied for all paths, but the middle one has zero intensity. This happens because there are two wave mixing process occurring on the same path, but interfering destructively. This interplay between path and polarization enabled an opportunity for all-optical switching.

Scalar structured light

The fields in Eq. (3) can be expanded in the well known spatial modes, and by using orthogonality relations, the right-hand side of this equation becomes a set of three mode overlap integrals. The modal description of this process has resulted in a important result regarding the interaction of light with matter, for example, the conservation of OAM per photon in classical[36,51] and quantum[37] nonlinear processes.

Interestingly, the coupling is not only between light and matter, but between differences in structure of the fields themselves, particularly within a given family. For instance, the "untwisting" of the azimuthal phase of an OAM Laguerre-Gaussian (LG) mode in turn altered the radial index[52,53], with the rules governing this interaction only recently unveiled[54], and shown to be true for wave mixing processes of any order[55]. This intricate relation is illustrated in Fig. 2(c). The first row shows a process where two different radial structures are used as inputs and the state generated ends up as a superposition of different radial orders, up to a mode of order equal to the sum of the input orders. On the second row, the azimuthal phases cancel each other, generating higher radial orders. Similar processes have been observed with Hermite-Gaussian (HG) modes. Here, their separable Cartesian form makes the interpretation of the selection rules far more straightforward, aided further by the fact that they are the natural solutions of the anisotropy of a biaxial crystal[56], an important aspect in optical cavities. Since these seminal studies, wave mixing with structured light has included Ince-Gaussian[57,58] and Bessel-Gaussian[59–62] modes, confirming OAM conservation and exploring the selection rules of these families. OAM conservation was not only shown for integer but also for fractional topological charges[63,64], in an off axis configuration[65] and even in plasmonic media[66–68]. A summary of the different behaviours structured light and its different modes can have in second order nonlinear wavemixing are summarized in Table 1.

One might ask if there is there a recipe for the input to the nonlinear process in order to obtain a desired output structured field? The answer can be trivial, where one or more of the input profiles are plane waves and one of them contains the desired structure. By this approach, LG and HG structured modes have been created, as well as general structured images[71]. When this is not possible, the HG basis is suggested to be optimal[72], and has been used for high fidelity mode generation[73]. Because wave mixing allows for light modulation by light, the process can be adapted to be used as a detector of structured light[71,74,75], and has been used to detect LG and HG modes with very little modal cross-talk, in a manner analogous to modal decomposition[76]. Even complex images can be handled in this manner, with the benefit of noise reduction (squaring a signal will amplify the strong and the decrease weak). For this reason, this has been an emerging application of SHG, with demonstrations including augmented edge contrast[77,78] and contrast enhancement to improve recognition of human faces and QR codes[79].

Vectorial structured light

So far we have considered the case where the structured

Table 1 | Behaviour of various structures of light in second order nonlinear wave mixing. Here, n_x/n_y are the indices for HG modes, ℓ, p are the azimuthal/radial indices for LG modes and p/m are the parameters for Ince-Gaussian modes. Indices with primes, such as ℓ'' are of fundamental field modes and the ones without are of the frequency generated.

Structure	Behaviour observed	Relations
Laguerre-Gaussian	OAM operations[36,47,51] Radial selection rule[53,54]	$\ell = \ell' + \ell''$ $p \leq p' + p(\ell' \times \ell > 0)$ $p \leq \min(\lvert\ell'\rvert, \lvert\ell\rvert) + p' + p(\ell' \times \ell < 0)$
Hermite-Gaussian	Independent selection rules[56] Optimal base for conversion[72]	$n_x \leq n'_x + n''$ (mod 2) $n_y \leq n'_y + n''_y$ (mod 2)
Ince-Gaussian	DoF coupling [57]	$p \leq p' + p''$ (mod 2) $m_0 \leq m \leq p$ (mod 2)
Helical Ince-Gaussian	OAM conservation [57]	$p \leq p' + p''$ (mod 2) $m_0 \leq m \leq p$ (mod 2) $m_{\mathrm{Net}} = m' + m''$
Bessel-Gaussian	OAM doubling in SHG[59] Transverse wavenumber superposition [60]	$\ell = 2\ell'$ $k_\perp = 2k'_\perp$
Bessel bottle beams	Self-healing and divergence increase [62]	-
Airy beams	Focusing distance related to wavelength Vortex phase preservation(Ring-Airy)[120] Direction switching in DFG[121]	- -
Fractional OAM	Topological charge transfer [122] Birth of vortex and creation of radial orders [63]	- -
Anti-chiral vortices	Radial-azimuthal coupled diffraction [55]	-
Vector beams	Polarization singularity doubling in SHG [82] Faithful frequency conversion [69] Phase conjugation in StimPDC [90]	- - -

light is scalar, so that the polarization is homogenous across the field. A complex vectorial structure is achieved by combining orthogonally polarized states such that each has its own unique spatial mode. If the spatial modes are also orthogonal, then the polarization structure of the field will be maximally inhomogeous[3]. On the right-hand side of Fig. 1(a) we have an example of a vector beam with spin-orbit coupling. Two beams of orthogonal circular polarization states and opposite OAM are combined to form a complex polarization pattern. The yellow lines represent the linear polarization state at every point in the transverse profile at a given angle. Since nonlinear wave mixing depends on both the spatial mode and polarization DoFs, it might seem that a inhomogenous polarization structure would be bound to change when frequency converted. In fact, frequency conversion of vector structured beams has been characterized as producing non-trivial scalar patterns in type-II SHG[80,81] and having an altered vector structure when generated in SHG with sandwiched crystals[82] and using a Sagnac loop[83]. In this sense, the inhomogeneous state of polarization has been proposed as a control parameter for nonlinear process[50,84]. Recently an elegant approach was realized using a Sagnac loop, making it possible to convert a vector beam in frequency[69,85,86] while retaining the polarization structure, as illustrated in Fig. 2(d). Here, one input is a vector beam and the other a auxiliary beam, the latter having a somewhat flat intensity and phase distribution. A polarizing beamsplitter (PBS) is used to separate the vector beam into two components where the loop shape makes them propagate in opposite directions. By inserting a half-wave plate (HWP) in the loop, each component of the vector beam is combined with an orthogonally polarized co-propagating plane wave, which enables faithful frequency conversion of each component independently. Lastly, the same PBS recombines both components back into a vector beam with the same spatially structured polarization but at a converted wavelength. Some observed effects of vector beams in wave mixing process are summarized in Table 1. The examples provided only deal with second order processes. A theoretical approach was already proposed to characterize the full vectorial nature of wave mixing for every nonlinear process order, based on input and output fields[87], but has yet to be realised.

A peculiar effect observed in the nonlinear regime is phase conjugation, where the generated beam has the conjugate (negative) phase of a impinging beam. The allure of the nonlinear approach is that no knowledge of the initial phase is required for the process, unlike linear phase conjugation that always requires some wavefront sensing and adaptive control. In nonlinear optics this effect was first achieved and historically associated with four-wave mixing, but it has been shown that a second order effect, Stimulated Parametric Down Conversion, can partially achieve it, conjugating the transverse phase structure[88] but not the propagation direction. It has been demonstrated with scalar[89] and as well as vector[90–92] beams.

Spin-orbit coupling

In paraxial optics, the spin angular momentum and the orbital angular momentum of a photon are treated as independent degrees of freedom. But even in this regime, we can find instances of these two quantities coupled. A notable example is a special group of vectorial inhomogeneous beams made of spatial modes carrying different OAM in polarization components carrying SAM. Besides these vector vortex beams, conical diffraction[93] has been shown to produce optical vortices in the linear regime depending on the input SAM, effectively coupling them. Conical diffraction is a consequence of birefringence and has been reported to excite second harmonic generation in biaxial crystals[94–96]. The combination of conical diffraction with nonlinear process such as second harmonic generation can be combined to create cascaded processes that operate both on OAM and SAM[97]. In this interesting example, the SAM is converted into OAM by conical diffraction, but only partially. The two parts (converted and unconverted) then act as fundamental fields for a SHG process of each state. The resulting beams from this conversion also suffer conical diffraction, having their OAM altered according to their SAM. By starting with a simple Gaussian beam with SAM, the authors show these two DoFs can be strongly coupled even in a simple material. However, these two degrees of freedom, while independent and possibly coupled, can interact in a nonlinear process[70], as depicted in Fig. 2(e). A spin-orbit coupled beam of OAM ℓ_ω is combined inside the crystal with another beam only having SAM S_ω, resulting in the generation of a beam having OAM $\ell_{2\omega} = \ell_\omega + S_\omega$.

Intra-cavity dynamics

Lasers are a well known nonlinear device, and here too structured light laser cavities have a long history (see ref.[98] for a review), with internal frequency generation used extensively for OAM generation[99] and even with wavelength tuneability[100]. While a full review is beyond the scope of this article (see refs.[98–100] for good reviews), we briefly highlight some interesting advances. These include intra-cavity geometric phase[101] for helicity control, spin-orbit effects[102] with high purity, vortex OPOs[103] to move into the mid-infrared, wavelength and OAM tuneable lasers[104] based on fibre geometries. Most of these solutions have been at low power. Nonlinear laser amplifiers have been used to raise the power levels, both in bulk crystals[105] and disks[106] with vectorial light, including parameteric amplification of ultrafast structured light[107], and with scalar structured light in Erbium fibre amplifiers[108] as well as by Raman amplification[109].

Frequency converting cavities for structured light at the source include the use of exotic intra-cavity elements such as spatial light modulators for radial modes[110] and metasurfaces for super-chiral OAM modes[111], with recent work extending to vortex lattices[112] and Poincaré beams[113]. Nonlinear optical elements are often placed in cavities to enhance the efficiency, but this too can influence modal structure. Nonlinear cavities such as Optical Parametric Oscillators (OPOs) show rich behaviour not seen in free-space propagation. For example, controlling the spatial properties of a Gaussian pumped triple resonant OPO changes its threshold and allows for simultaneous oscillation of several mode pairs with fixed relative phases[46], and can result in multiple complex patterns[114,115]. A thorough study on the influence of the geometrical properties of the OPO on the generated spatial modes can be seen in[116] and their applications in continuous variable entanglement in[117]. The structured output can be tailored by structuring the pump[56,118], as can the geometry of the cavity itself[119], making the cavity selective to specific modes.

Structured matter for structured light

The nonlinearity we are discussing refers to the interaction of light and matter. The structure of the output light (created or detected) is therefore tailored by both the input light and the medium, allowing the latter to be tailored. This is achieved when the medium higher-order susceptibility is no longer a constant but instead has a space dependency, e.g., $\chi^{(2)}(\boldsymbol{r})$ for the second order term. The structuring of the medium can be a very important tool to shape the outcome of a nonlinear process. We will now present two of the more prominent structured media in the field: crystals and metasurfaces.

Crystals

In the past this structuring of crystals has been done through acousto-optic modulators, giving rise to effects such as Bragg and Raman-Nath scattering, modulating the refractive index hence the phase matching conditions as well. The modern toolkit includes more direct manipulation of materials (e.g., structured photonic crystal). Phase matching in nonlinear photonic crystals has been well explained and explored[123–125] with periodic poling playing a important role in the past decade[126], branching into many applications, including a nonlinear version of the Talbot effect[127]. By introducing a carefully crafted spatial modulation in a nonlinear crystal, it was shown to be possible to control the amplitude and phase of the generated fields[128–130]. One highlight is the work illustrated in Fig. 3(a) where the authors carefully exploit the inversion of dipole domains to "twist" light as it is created[130]. At any point in the fundamental beam's spatial profile there is light conversion with the same efficiency, but not the same phase. This phase modulation acts as a medium-enabled nonlinear holography.

The phase-matching conditions involves not only material but also energy constrains. The periodic polling can not only enable frequency control[131,132] but when multiplexed it achieves phase-matching for multiple wavelengths in the same crystal[133]. Recently, a novel pattern in the periodic polling named quasi-periodic polling achieved simultaneous second and third harmonic generation[134]. Further, the structuring of the media is not restricted to one dimension: by using oblique incidence on a periodically polled crystal it was possible to couple mode selection with phase matching[135], coupling DoFs of light and matter. Photonic crystals can be structured so that phase-matching is crafted in both longitudinal and transverse directions[136–138] so that light is structured as it is generated. A thorough review on this emerging area can be seen in ref.[139].

An interesting combination of birefringence and periodic polling can be seen in ref.[140], where the spatial macroscopic structure complements the unit cell structure to achieve both type-0 and type-II phase-matching simultaneously. Besides changing the structure itself, changing the orientation of the medium can achieve interesting results. The sandwich crystal configuration (a combination of two identical crystals optically joined but oriented at 90°) has been employed for the frequency conversion of vector light[82].

As much as the structured of the medium dictates

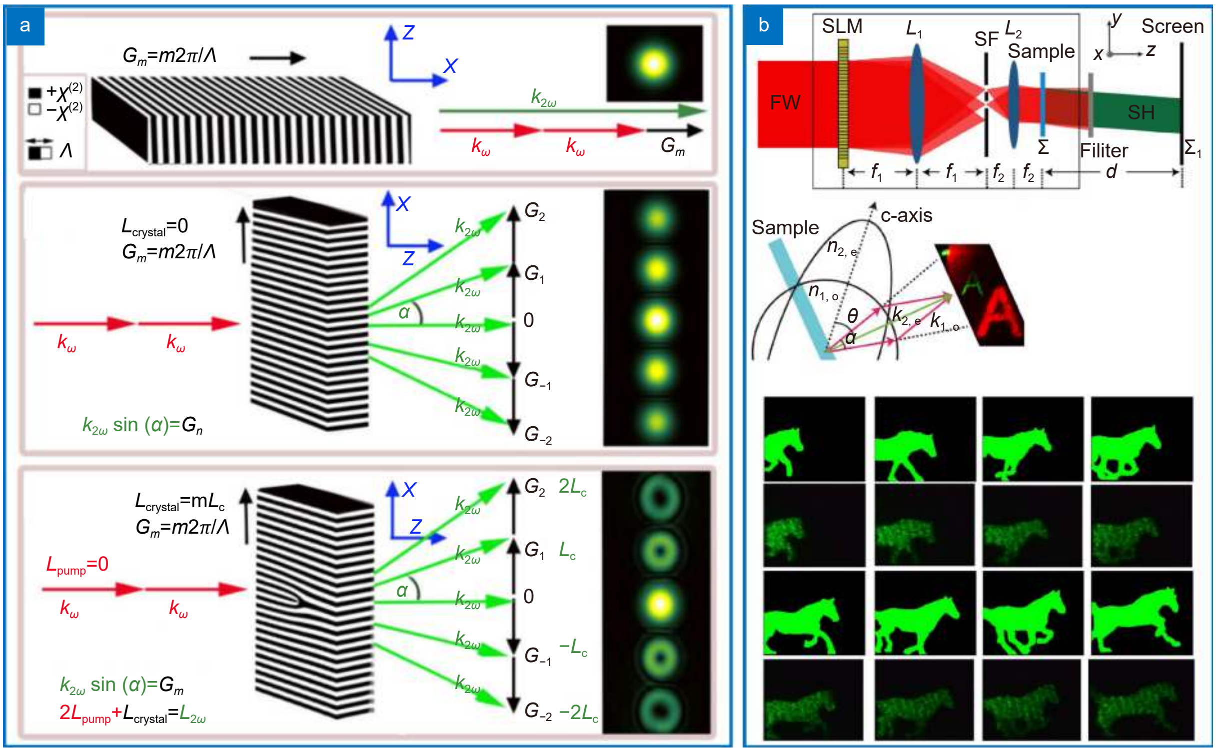

Fig. 3 | Nonlinear Holography. In (**a**) the structuring of the medium is illustrated: the fundamental field is always the same, but the medium is not. The selective inversion of the electric domain across the transverse plane creates different spatial structures in the second harmonic field. The periodical transverse structure is responsible for multiple phase matching mechanisms, both longitudinally and transversely. In (**b**) it is shown how non-collinear SHG can transfer a specific intensity pattern from one wavelength to the other. First row shows the imaging arrangement and the second column shows the phase-matching conditions and an example of output modes. Right below is a experimental demonstration that this can be used for real-time frequency conversion of computer generated holograms. Figure repoduced from: (a) ref.[130], © American Physical Society; (b) ref.[158], © Optica Publishing Group.

phase-matching, the other way around also happens: we can use this property of the medium from a material analysis perspective[141] and use these nonlinear process to characterize crystals according to their symmetry groups[142].

Metasurfaces

The structuring of the medium is not exclusive to crystals, as metasurfaces have been employed in many areas and nonlinear optics is no exception. They have seen a lot of atention recently by achieving high conversion efficiencies. The nanostructures composing these crafted surfaces are capable of confining light in volumes smaller than the diffraction limit[145,146], greatly enhancing nonlinear effects. Excellent reviews can be found in ref.[145,147,148]. They are structured by definition and can combine wavelength conversion with wavefront control[149−151], spin-orbit interactions[152], OAM operations involving SAM[143], image encoding[153] and optical activity[154]. Two illustrative cases can be highlighted: OAM-SAM interactions[143] and metalensing[144]. By creating gold meta-atoms with three-fold symmetry, the authors in ref.[143] arranged the metasurface to enable azimuthal geometric phase and frequency conversion at the same time, creating devices depicted in Fig. 4(a) that operates on both SAM and OAM. In the second one, illustrated in Fig. 4(b), the authors combine a novel technique that exploits Mie ressonance in all-dielectric metasurfaces and third harmonic generation. The phase of the generated wave inherits a metalens profile from the medium structure. This results in a process that illuminates an aperture with light of a given wavelength and then, after passing through the metasurface, it is converted to its third harmonic and imaged at a focal point. All in a flat and compact optical component. The development of metasurfaces has allowed tremendous growth in nonlinear optics, not only because of their high efficiency, but their fabrication process being scalable and the high damage threshold needed for laser sources integration. In ref.[111] the authors demonstrate how a metasurface placed inside a laser cavity can generate high purity OAM modes from the source, depicted in Fig. 4(c).

Nonlinear holography

Since very early in the study of nonlinear optics, it was understood that wave mixing meant modulation and that this could be used for holography[155]. In the original version, the counter-propagating fields involved in the four-wave mixing formed a grating that changed the generated field. Nowadays, we have more advanced forms of holography. When looking at Eq. (3), it is clear that all fields involved in wave mixing influence each other in amplitude and phase. But more importantly, it has come to a collective understanding: the optical field involved in wave-mixing can be seen as *diffracted by the other involved fields*. Going back to Eq. (3) we can set $E_1^{(\omega_1)}$ to be a plane wave and $E_2^{(\omega_2)}$ a diffraction pattern, both in a non-depleting regime happening only at a single plane in propagation. This would generate a field $E_3^{(\omega_3)}$ not different than a simple plane wave passing through the same diffraction obstacle.

In this sense, by shaping the fundamental beam as a hologram it is possible to modulate the generated beam as it is created[156]. This process allows for holograms that are self adaptive and depend on the generating fields, being able to copy or regenerate optical modes[157], even complex patterns in real time[158]. In this example, illustrated in Fig. 3(b), the authors generate a hologram and the light affected by it is filtered in the Fourier domain. Only the first order, containing the intended pattern, and the zero-th order, containing a Gaussian profile, are selected. Those are used as inputs for non-collinear SHG, and the result in the intermediate path is the frequency conversion of any pattern encoded in the hologram in real time. The authors demonstrate this by encoding the holograms with frames of a movie of a running horse in a infrared laser and detecting the same frames on the visible green light.

If the interaction happens in more than a single plane, i.e. the medium is longer than a diffraction length, these approaches can be extended to three dimensions for volume holography[159,160] in nonlinear crystals, and the reader is referred to refs.[161−163] for excellent reviews on this topic.

Four-wave mixing

As we consider higher-order nonlinear effects,

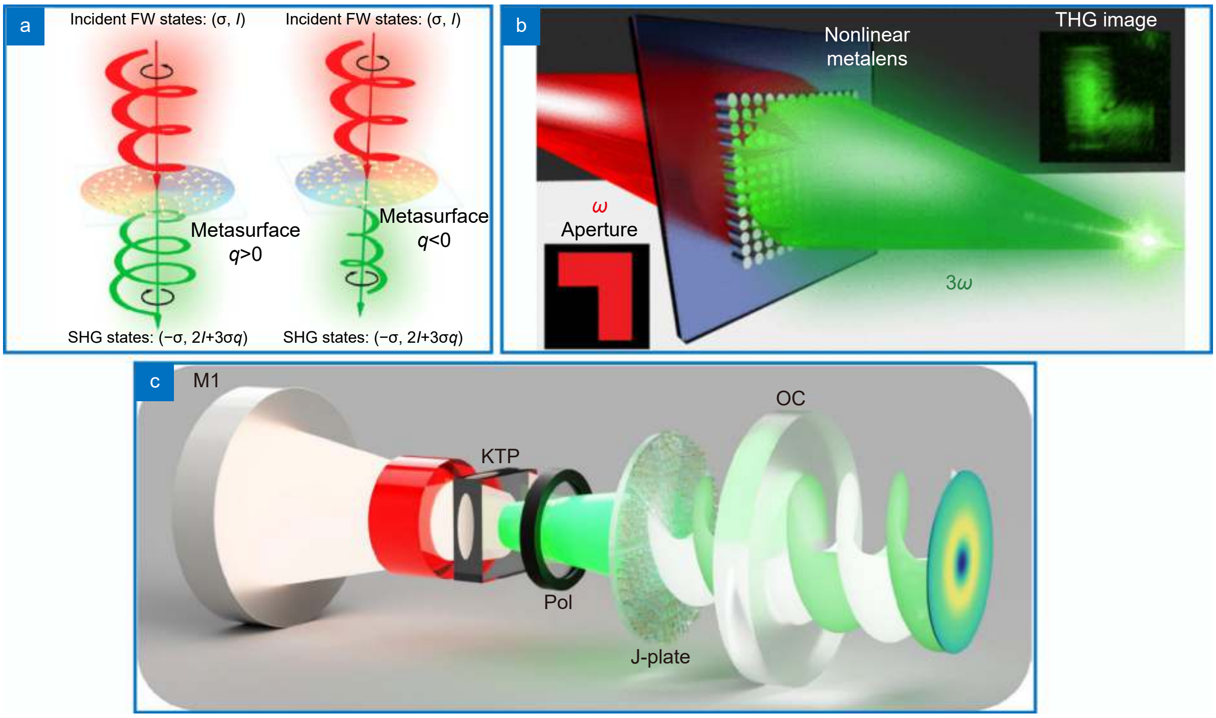

Fig. 4 | Nonlinear optics enabled metasurfaces. These devices were shown to enable non-trivial interactions while frequency converting beams. In (**a**) a SHG process coupling SAM and OAM. The combination of frequency conversion with holography creates metasurfaces with metalensing properties in (**b**)[144]. An application taking advantage of the high damage threshold of these materials can be seen in (**c**)[111] where the inclusion of a metasurface inside an optical cavity creates a laser with OAM from the source. Figure repoduced with permission from: (a) ref.[143], © American Chemical Society; (b) ref.[144], under a Creative Commons Non-Commercial No Derivative Works (CC-BY-NC-ND) Attribution License; (c) ref.[111], Springer Nature.

wave-mixing becomes increasingly complex. For example, OAM conservation in a four-wave mixing (FWM) process with third order nonlinearity was observed in cold cesium gas in ref.[164] where only one beam was structured with OAM, resulting in the transfer of OAM to the generated beam and similarly with modal superposition[165]. This was later expanded to include both probe and pump having OAM[166,167], where the phase matching conditions can be fulfilled in more directions than lower order process and this results in the creation of a higher number of states created in different paths, as depicted in Fig. 5(a). Beyond OAM, a hot atomic vapour of ^{85}Rb was used to generate Bessel beams from Gaussian pumps by careful control of the phase matching[168]. With the same medium, a multimode four-wave-mixing process was established with two pump beams of the same frequency that crossed at a small angle, producing three photons that are highly correlated and could be applied to multipartite entanglement distribution[169]. The idea exploited the simultaneous fulfillment of two phase matching conditions that reinforce one another.

Using a long medium approximation, radial and angular mode conversion by FWM in a heated Rb vapour was demonstrated, making evident the role of the Gouy phase-matching in this regime[170]. Beyond just spatial DoFs, the spatial and temporal DoFs are not independent in this process[171], where frequency control enables selection of various spatial modes as outputs.

Recent developments with dielectric materials have been shown to enable four-wave mixing with high efficiency. These materials have been crafted in the nanoscale as plasmonic nanoantennas[172,173], metasurfaces[145–148], nanodisks[174], enabling not only frequency conversion to a wider range of wavelengths but the intrinsic structure also motivated simultaneous wavefront shaping[144].

High-harmonic generation

High-harmonic generation (HHG) is an extreme process, not regarded as perturbative process and cannot be represented in Eq. (2). This can be seen phenomenologicaly by the fact that all harmonics generated have comparable efficiencies, unlike parametric frequency conversion. Instead, HHG is defined by the ionization of the medium: light impinging in a medium is strong enough that it perturbs an electron bound to an atomic system to the point where it escapes its bounding potential. When this electron is recaptured by an identical atomic system, it liberates the kinetic energy stored, emitting a photon of an energy many times the absorbed ones. This description is known as the recombination model[175]. The different underlying physics makes this process still a mystery to be studied in the context of structured light interaction with matter. In recent years, there has been considerable progress tackling this problem. One might wonder if OAM would be conserved or how SAM would affect this process. A few studies observed that the polarization of the impinging light can be controlled[176] even at isolated pulses timescale[177]. Regarding the spatial structure, some previously unseen behaviour was demonstraded. When using optical phase vortices, OAM operations happen periodically (along harmonic order)[178]. Analogous to phase matching conditions in a non-collinear parametric process, it was possible generate many other beams with just two inputs having differing OAM[179], demonstrating OAM algebra. Not only the azimuthal degree of freedom was studied, but the radial structure was also studied in ref.[180] to show its dependency on the atomic dipole phase. An exciting application is the control of generated spectral domain via structuring the pump to generate an effective blazed active grating in gases[181,182] and the generation of autofocusing intense beams[183]. While these studies were done separate, others show that these two DoF are not independent in this process and use polarization as a control parameter of this process[184,185]. Since the output was made of many different frequencies with different OAM, this effect was characterized as producing Spatio-Temporal vortex in extreme UV[186] and even self-torque, a behaviour previously not seen in light[187].

Space-time coupling

The medium cannot interact instantly with light: first, structured light interacts with a medium that inherits this structure momentarily. When the first light source is no longer there, a second light source interacts with the medium and inherits the structure of the first one. This effect is known as optical memory and is regarded as a possibility for storing quantum information in a multidimensional state space. A demonstration of this principle was observed in ref.[188], where light interacting with an atomic system (cold cesium gas) induced by a coherence grating lead to OAM conservation, a first step towards the demonstration of optical storage. This spatially dependent coherence transferred to the medium was shown be maintained in time[189], reporting storage times of up to 100 μs. It was shown in ref.[190] that it is possible to store OAM in the same system and also retrieve it by employing Bragg diffraction. The same effect was also achieved in ref.[191] but exploiting a different effect: coherent population oscilation, which uses the long relaxation time of the ground state of an open two-level system to store information carried by a light field. This process is depicted in Fig. 5(b), where a writting stage is the interference of two beams carrying opposite OAM inside the medium. The reading stage is a Gaussian beam that enters the medium and exits with information from a beam which was no longer there. In Fig. 5(c) it is shown that different nonlinearity orders exhibit different time signatures, which can be used as a control mechanism[192]. Advancing on the path of long lived optical memory storage, by exploring electromagnetic induced transparency, in ref.[193] the authors were able to execute OAM storage and retrieval as a reversible process

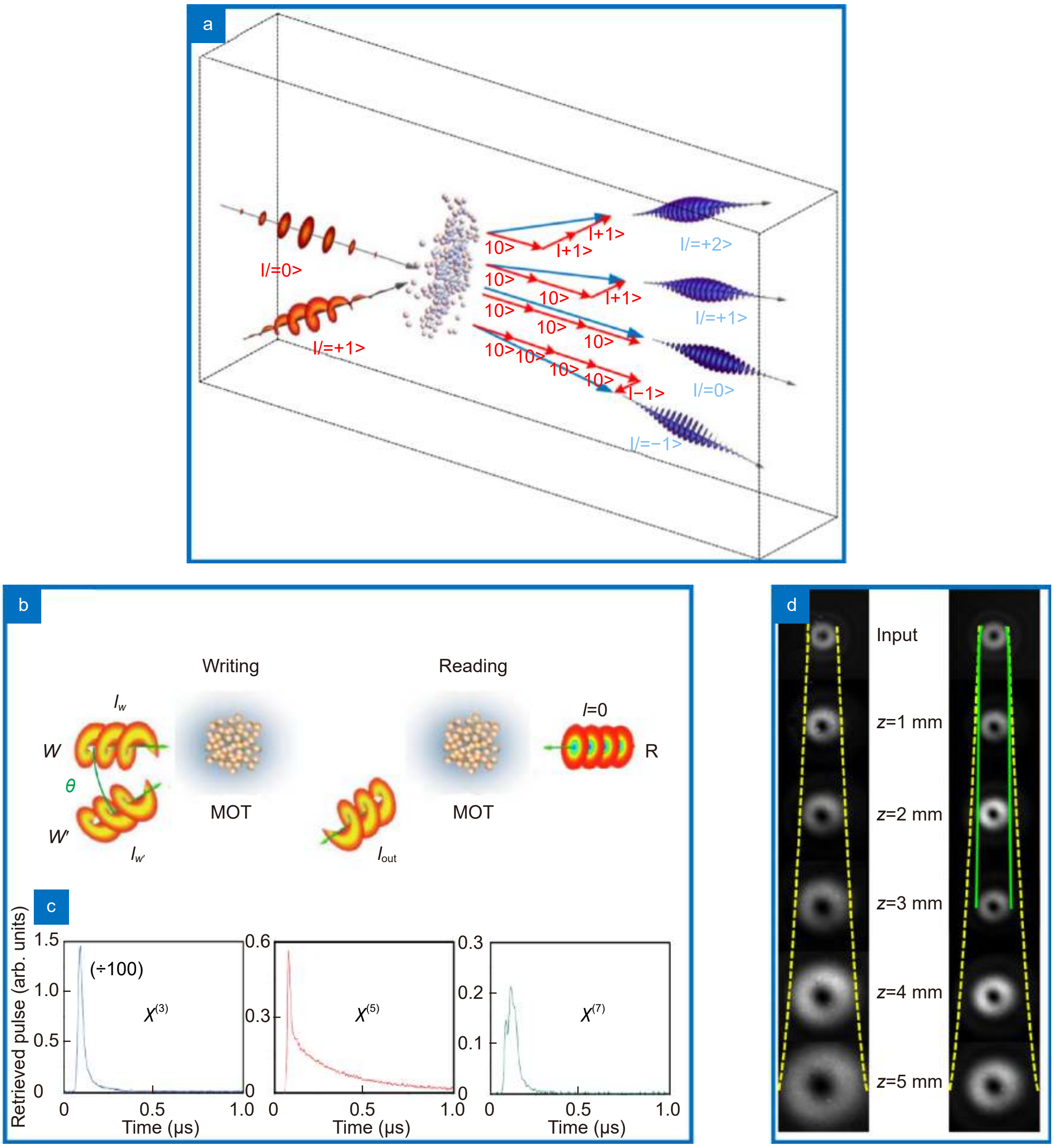

Fig. 5 | Higher order process. In the generation of high harmonic orders, it is possible to generate beams of many different OAM from just two different inputs, as depicted in (**a**). The process of writting and reading optical memory is depicted in (**b**) and the diference in time scales depending on the order of the nonlinear process in (**c**). In (**d**) it is demonstrated robust self-trapping of a bright vortex beam by exploiting higher order nonlinearities of odd orders. Figure repoduced from: (a) ref.[209], Springer Nature; (b) ref.[191], © Optica Publishing Group; (c) ref.[192], © Optica Publishing Group; (d) ref.[204], © American Physical Society.

in single photon level.

While the process described above couples a specific structure to another during a time window, there are light structures that are notorious for having its time and space non-separable: the spatiotemporal optical vortices[14,194]. These beams exhibit OAM transverse to propagation direction, instead of usual longitudinal OAM of phase vortex beams. One might wonder if these space-time structures would hold in the nonlinear regime. Recent works showed that in SHG the spatiotemporal OAM is also conserved[195,196], while also reporting effects such as time astigmatism and singularity splitting due to group-velocity dispersion.

Spatial solitons

The self-focusing action of a medium can balance precisely the diffraction of a beam, resulting in the creation of optical solitons. The first observed optical solitons were dark vortex solitons, which are phase vortices that propagate in a self-defocusing medium with third order nonlinearity $\chi^{(3)} < 0$[197]. This means that the beam modulate itself, with a defocusing effect shaped across the transverse plane by the intensity profile. The dark central of a vortice would naturally increase due to propagation, but a self-defocusing effect in the bright regions would redistribute the intensity of the ring back to the center. The balance of these two process creates a dark soliton: a dark region that does not diffract in propagation.

On the other hand, bright phase vortices suffer from azimuthal modulation instability in self focusing media, which results in their splitting and thus, were hard to be observed. This type of instability in the transverse modulation is similar to one responsible on the filamentation of beams and generation on trains of optical solitons[198].

However, by using non-centrosymetric metal-dielectric nanocomposites, higher-order nonlinear effects such as fifth and seventh order become dominant and cause self-phase modulation[199,200]. This ultimately allowed for the observation of stable bright vortex solitons in ref.[201−204]. In Fig. 5(d) this is illustrated in two columns: lower intensity (left) and higher intensity (right). For lower intensities, the natural diffraction of the beam propagation happens as usual as the beam size increases in propagation. For higher intensities, the beam size stays roughly the same in a short propagation distance inside this medium. This happens because the self-modulation effect is caused by nonlinear polarization of odd orders which alternate in sign. The lower orders can saturate, so by increasing intensity, the higher orders nonlinear effects becomes dominant and balances defocusing with focusing. For more detailed information, excellent reviews are found in refs.[205−208].

Quantum regime

Nonlinear processes have long been associated with quantum optics as the source of entangled photons. The most common source of entangled photons is Spontaneous Parametric Down Conversion (SPDC)[210], a nonlinear process at its core. By harnessing entanglement and the transverse structure of the photons it is possible to increase the dimensions of quantum protocols[6]. This is often achieved by post-selecting a particular state, the choice of which affects the bi-photon entanglement spectrum in both its shape and dimensionality. This was first realized using OAM[37] and subsequently many transverse structures were studied[211−215], as well as inhomogenously polarized beams[92,216] and multi-path schemes[217,218]. Soon after it followed that it was possible to engineer the pump profile to manipulate the bi-photon spectrum and generate a entanglement spectrum straight out of the source[219−223]. Beyond nonlinear optics for creation, the detection and control of quantum states by nonlinear processes has been far less studies, and very much in its infancy.

Although quantum technologies have experienced rapid development in recent years, with light playing a key role, this has mostly been restricted to linear optical solutions, e.g., the ubiquitous beam splitter. For optical systems, a photon-photon interaction in vacuum is not possible. While this is partially true in matter as well, we observe in the nonlinear regime a photon-photon interaction mediated by the medium. Unfortunately this interaction is very unlikely to happen, but it does not mean impossible as this mixture have seen important advances recently (see ref.[224] for a good review), with the building block of single photon wave mixing[225]. Nonlinear optics have been suggested in various quantum processes[226−229] and even used for Bell filters[230] for polarization, entanglement swapping[231] and a quantum repeater device[232,233]. Only recently has structured light entered the equation, with a nonlinear version of spatial teleportation demonstrated with up to 10 modes, overcoming the significant hurdle of ancilliary photons and settting a new state-of-the-art of 10 dimensional teleportation[234].

Conclusion

In this review we have touched many topics regarding nonlinear optics with structured light. Unlike linear optics, which generally act on only one degree of freedom, these process have the intriguing feature of coupling many DoFs through the properties of the medium. The possibility is for compact solutions for the creation, control and detection of structured light, yet many open questions remain: what structures can we create? How can we transfer structures within and between DoFs? What is the exact input one would need to generate a specific desired output? These questions are still open even in the lowest order of wave mixing. As new light-matter interactions are discovered in the nonlinear regime, it is exciting to see how their structures couple and what insights can be deduced.

From real time holographic transmission to optical memory effects, from bulk crystalline media to sparse gas jets, there are many physical phenomena that are nonlinear optical processes. The development of new materials, techniques and interactions, alongside ever more powerful laser sources, all signal an exciting future for nonlinear control of structured light, and structured light control of nonlinear processes.

References

1. Forbes A, de Oliveira M, Dennis MR. Structured light. *Nat Photonics* **15**, 253–262 (2021).
2. Otte E, Alpmann C, Denz C. Polarization singularity explosions in tailored light fields. *Laser Photonics Rev* **12**, 1700200 (2018).
3. Rosales-Guzmán C, Ndagano B, Forbes A. A review of complex vector light fields and their applications. *J Opt* **20**, 123001 (2018).
4. Willner AE, Huang H, Yan Y, Ren Y, Ahmed N et al. Optical communications using orbital angular momentum beams. *Adv Opt Photonics* **7**, 66–106 (2015).
5. Padgett MJ. Orbital angular momentum 25 years on [Invited]. *Opt Express* **25**, 11265–11274 (2017).
6. Forbes A, Nape I. Quantum mechanics with patterns of light: progress in high dimensional and multidimensional entanglement with structured light. *AVS Quantum Sci* **1**, 011701 (2019).
7. Erhard M, Fickler R, Krenn M, Zeilinger A. Twisted photons: new quantum perspectives in high dimensions. *Light Sci Appl* **7**, 17146 (2018).
8. Larocque H, Sugic D, Mortimer D, Taylor AJ, Fickler R et al. Reconstructing the topology of optical polarization knots. *Nat Phys* **14**, 1079–1082 (2018).
9. Galvez EJ, Rojec BL, Kumar V, Viswanathan NK. Generation of isolated asymmetric umbilics in light's polarization. *Phys Rev A* **89**, 031801 (2014).
10. Zdagkas A, Shen YJ, McDonnell C, Deng J, Li G et al. Observation of toroidal pulses of light. arXiv: 2102.03636 (2021).
11. Keren-Zur S, Tal M, Fleischer S, Mittleman DM, Ellenbogen T. Generation of spatiotemporally tailored terahertz wavepackets by nonlinear metasurfaces. *Nat Commun* **10**, 1778 (2019).
12. Bauer T, Banzer P, Karimi E, Orlov S, Rubano A et al. Optics. Observation of optical polarization Möbius strips. *Science* **347**, 964–966 (2015).
13. Dallaire M, McCarthy N, Piché M. Spatiotemporal Bessel beams: theory and experiments. *Opt Express* **17**, 18148–18164 (2009).
14. Chong A, Wan CH, Chen J, Zhan QW. Generation of spatiotemporal optical vortices with controllable transverse orbital angular momentum. *Nat Photonics* **14**, 350–354 (2020).
15. Kondakci HE, Abouraddy AF. Diffraction-free space-time light sheets. *Nat Photonics* **11**, 733–740 (2017).
16. Shen YJ, Hou YN, Papasimakis N, Zheludev NI. Supertoroidal light pulses as electromagnetic skyrmions propagating in free space. *Nat Commun* **12**, 5891 (2021).
17. Shen YJ, Nape I, Yang XL, Fu X, Gong ML et al. Creation and control of high-dimensional multi-partite classically entangled light. *Light Sci Appl* **10**, 50 (2021).
18. Shen YJ, Yang XL, Naidoo D, Fu X, Forbes A. Structured ray-wave vector vortex beams in multiple degrees of freedom from a laser. *Optica* **7**, 820–831 (2020).
19. Spreeuw RJC. A classical analogy of entanglement. *Found Phys* **28**, 361–374 (1998).
20. Ndagano B, Perez-Garcia B, Roux FS, McLaren M, Rosales-Guzman C et al. Characterizing quantum channels with non-separable states of classical light. *Nat Phys* **13**, 397–402 (2017).
21. Forbes A, Aiello A, Ndagano B. Classically entangled light. *Prog Opt* **64**, 99–153 (2019).
22. Aiello A, Banzer P, Neugebauer M, Leuchs G. From transverse angular momentum to photonic wheels. *Nat Photonics* **9**, 789–795 (2015).
23. Padgett MJ, Courtial J. Poincaré-sphere equivalent for light beams containing orbital angular momentum. *Opt Lett* **24**, 430–432 (1999).
24. Milione G, Sztul HI, Nolan DA, Alfano RR. Higher-order poincaré sphere, stokes parameters, and the angular momentum of light. *Phys Rev Lett* **107**, 053601 (2011).
25. Shen YJ. Rays, waves, SU(2) symmetry and geometry: toolkits for structured light. *J Opt* **23**, 124004 (2021).
26. Mazilu M, Stevenson DJ, Gunn-Moore F, Dholakia K. Light beats the spread: "non-diffracting" beams. *Laser Photonics Rev* **4**, 529–547 (2010).
27. Gossman D, Perez-Garcia B, Hernandez-Aranda RI, Forbes A. Optical interference with digital holograms. *Am J Phys* **84**, 508–516 (2016).
28. Ayuso D, Neufeld O, Ordonez AF, Decleva P, Lerner G et al. Synthetic chiral light for efficient control of chiral light-matter interaction. *Nat Photonics* **13**, 866–871 (2019).
29. Maiman TH. Stimulated optical radiation in ruby. *Nature* **187**, 493–494 (1960).
30. Franken PA, Hill AE, Peters CW, Weinreich G. Generation of optical harmonics. *Phys Rev Lett* **7**, 118–119 (1961).
31. New GHC, Ward JF. Optical third-harmonic generation in gases. *Phys Rev Lett* **19**, 556–559 (1967).
32. Simon HJ, Bloembergen N. Second-harmonic light generation in crystals with natural optical activity. *Phys Rev* **171**, 1104–1114 (1968).

33. Abraham NB, Firth WJ. Overview of transverse effects in nonlinear-optical systems. *J Opt Soc Am B* **7**, 951–962 (1990).
34. Basistiy IV, Bazhenov VY, Soskin MS, Vasnetsov MV. Optics of light beams with screw dislocations. *Opt Commun* **103**, 422–428 (1993).
35. Shen YJ, Wang XJ, Xie ZW, Min CJ, Fu X et al. Optical vortices 30 years on: OAM manipulation from topological charge to multiple singularities. *Light Sci Appl* **8**, 90 (2019).
36. Dholakia K, Simpson NB, Padgett MJ, Allen L. Second-harmonic generation and the orbital angular momentum of light. *Phys Rev A* **54**, R3742–R3745 (1996).
37. Mair A, Vaziri A, Weihs G, Zeilinger A. Entanglement of the orbital angular momentum states of photons. *Nature* **412**, 313–316 (2001).
38. Boyd RW. *Nonlinear Optics* 3rd ed (Elsevier, Oxford, 2008).
39. Murti YVGS, Vijayan C. *Essentials of Nonlinear Optics* (John Wiley & Sons, New York, 2014).
40. Shen YR. *The Principles of Nonlinear Optics* (John Wiley & Sons, New York, 1984).
41. Singh K, Buono WT, Chavez-Cerda S, Forbes A. Demonstrating arago-fresnel laws with Bessel beams from vectorial axicons. *J Opt Soc Am A* **38**, 1248–1254 (2021).
42. Zhou ZY, Li Y, Ding DS, Jiang YK, Zhang W et al. Generation of light with controllable spatial patterns via the sum frequency in quasi-phase matching crystals. *Sci Rep* **4**, 5650 (2014).
43. Shao GH, Wu ZJ, Chen JH, Xu F, Lu YQ. Nonlinear frequency conversion of fields with orbital angular momentum using quasi-phase-matching. *Phys Rev A* **88**, 063827 (2013).
44. Steinlechner F, Hermosa N, Pruneri V, Torres JP. Frequency conversion of structured light. *Sci Rep* **6**, 21390 (2016).
45. Li Y, Zhou ZY, Ding DS, Shi BS. Sum frequency generation with two orbital angular momentum carrying laser beams. *J Opt Soc Am B* **32**, 407–411 (2015).
46. Schwob C, Cohadon PF, Fabre C, Marte MAM, Ritsch H et al. Transverse effects and mode couplings in OPOS. *Appl Phys B* **66**, 685–699 (1998).
47. Buono WT, Moraes LFC, Huguenin JAO, Souza CER, Khoury AZ. Arbitrary orbital angular momentum addition in second harmonic generation. *New J Phys* **16**, 093041 (2014).
48. Roger T, Heitz JJF, Wright EM, Faccio D. Non-collinear interaction of photons with orbital angular momentum. *Sci Rep* **3**, 3491 (2013).
49. Bovino FA, Braccini M, Giardina M, Sibilia C. Orbital angular momentum in noncollinear second-harmonic generation by off-axis vortex beams. *J Opt Soc Am B* **28**, 2806–2811 (2011).
50. Buono WT, Santiago J, Pereira LJ, Tasca DS, Dechoum K et al. Polarization-controlled orbital angular momentum switching in nonlinear wave mixing. *Opt Lett* **43**, 1439–1442 (2018).
51. Courtial J, Dholakia K, Allen L, Padgett MJ. Second-harmonic generation and the conservation of orbital angular momentum with high-order Laguerre-Gaussian modes. *Phys Rev A* **56**, 4193–4196 (1997).
52. Pereira LJ, Buono WT, Tasca DS, Dechoum K, Khoury AZ. Orbital-angular-momentum mixing in type-II second-harmonic generation. *Phys Rev A* **96**, 053856 (2017).
53. Pires DG, Rocha JCA, Jesus-Silva AJ, Fonseca EJS. Higher radial orders of Laguerre-Gaussian beams in nonlinear wave mixing processes. *J Opt Soc Am B* **37**, 1328–1332 (2020).
54. Wu HJ, Mao LW, Yang YJ, Rosales-Guzmán C, Gao W et al. Radial modal transitions of Laguerre-Gauss modes during parametric up-conversion: towards the full-field selection rule of spatial modes. *Phys Rev A* **101**, 063805 (2020).
55. Buono WT, Santos A, Maia MR, Pereira LJ, Tasca DS et al. Chiral relations and radial-angular coupling in nonlinear interactions of optical vortices. *Phys Rev A* **101**, 043821 (2020).
56. Alves GB, Barros RF, Tasca DS, Souza CER, Khoury AZ. Conditions for optical parametric oscillation with a structured light pump. *Phys Rev A* **98**, 063825 (2018).
57. Pires DG, Rocha JCA, da Silva MVEC, Jesus-Silva AJ, Fonseca EJS. Mixing Ince-Gaussian modes through sum-frequency generation. *J Opt Soc Am B* **37**, 2815–2821 (2020).
58. Yang HR, Wu HJ, Gao W, Rosales-Guzmán C, Zhu ZH. Parametric upconversion of Ince-Gaussian modes. *Opt Lett* **45**, 3034–3037 (2020).
59. Jarutis V, Matijošius A, Smilgevičius V, Stabinis A. Second harmonic generation of higher-order Bessel beams. *Opt Commun* **185**, 159–169 (2000).
60. Ding DS, Lu JY. Second-harmonic generation of the *n*th-order Bessel beam. *Phys Rev E* **61**, 2038–2041 (2000).
61. Shinozaki K, Xu CQ, Sasaki H, Kamijoh T. A comparison of optical second-harmonic generation efficiency using Bessel and Gaussian beams in bulk crystals. *Opt Commun* **133**, 300–304 (1997).
62. Rao AS, Yadav D, Samanta GK. Nonlinear frequency conversion of 3D optical bottle beams generated using a single axicon. *Opt Lett* **46**, 657–660 (2021).
63. Pires DG, Rocha JCA, Jesus-Silva AJ, Fonseca EJS. Interaction of fractional orbital angular momentum in two-wave mixing processes. *J Opt* **22**, 035502 (2020).
64. Dai KJ, Miller JK, Li WZ, Watkins RJ, Johnson EG. Fractional orbital angular momentum conversion in second-harmonic generation with an asymmetric perfect vortex beam. *Opt Lett* **46**, 3332–3335 (2021).
65. Rao AS. Characterization of off-axis phase singular optical vortex and its nonlinear wave-mixing to generate control broad OAM spectra. *Phys Scr* **95**, 055508 (2020).
66. Zhdanova AA, Shutova M, Bahari A, Zhi MC, Sokolov AV. Topological charge algebra of optical vortices in nonlinear interactions. *Opt Express* **23**, 34109–34117 (2015).
67. Wadhwa J, Singh A. Second harmonic generation of self-focused Hermite-Gaussian laser beam in collisional plasma. *Optik* **202**, 162326 (2020).
68. Xiong XYZ, Al-Jarro A, Jiang LJ, Panoiu NC, Sha WEI. Mixing of spin and orbital angular momenta via second-harmonic generation in plasmonic and dielectric chiral nanostructures. *Phys Rev B* **95**, 165432 (2017).
69. Wu HJ, Zhao B, Rosales-Guzmán C, Gao W, Shi BS et al. Spatial-polarization-independent parametric up-conversion of vectorially structured light. *Phys Rev Appl* **13**, 064041 (2020).
70. da Silva BP, Buono WT, Pereira LJ, Tasca DS, Dechoum K et al. Spin to orbital angular momentum transfer in frequency up-conversion. *Nanophotonics* **11**, 771–778 (2021).
71. Sephton B, Vallés A, Steinlechner F, Konrad T, Torres JP et al. Spatial mode detection by frequency upconversion. *Opt Lett* **44**, 586–589 (2019).
72. Pires DG, Rocha JCA, Jesus-Silva AJ, Fonseca EJS. Suitable state bases for nonlinear optical mode conversion protocols. *Opt Lett* **45**, 4064–4067 (2020).
73. Fang XY, Kuang ZY, Chen P, Yang HC, Li Q et al. Examining second-harmonic generation of high-order Laguerre-Gaussian

modes through a single cylindrical lens. *Opt Lett* **42**, 4387–4390 (2017).

74. Kumar S, Zhang H, Maruca S, Huang YP. Mode-selective image upconversion. *Opt Lett* **44**, 98–101 (2019).
75. Zhang H, Kumar S, Huang YP. Mode selective up-conversion detection with turbulence. *Sci Rep* **9**, 17481 (2019).
76. Pinnell J, Nape I, Sephton B, Cox MA, Rodríguez-Fajardo V et al. Modal analysis of structured light with spatial light modulators: a practical tutorial. *J Opt Soc Am A* **37**, C146–C160 (2020).
77. Qiu XD, Li FS, Zhang WH, Zhu ZH, Chen LX. Spiral phase contrast imaging in nonlinear optics: seeing phase objects using invisible illumination. *Optica* **5**, 208–212 (2018).
78. Xu DF, Ma TL, Qiu XD, Zhang WH, Chen LX. Implementing selective edge enhancement in nonlinear optics. *Opt Express* **28**, 32377–32385 (2020).
79. Hong L, Lin F, Qiu XD, Chen LX. Second harmonic generation based joint transform correlator for human face and QR code recognitions. *Appl Phys Lett* **116**, 231101 (2020).
80. Zhang L, Qiu XD, Li FS, Liu HG, Chen XF et al. Second harmonic generation with full Poincaré beams. *Opt Express* **26**, 11678–1184 (2018).
81. Liu HG, Li H, Zheng YL, Chen XF. Nonlinear frequency conversion and manipulation of vector beams. *Opt Lett* **43**, 5981–5984 (2018).
82. Saripalli RK, Ghosh A, Chaitanya NA, Samanta GK. Frequency-conversion of vector vortex beams with space-variant polarization in single-pass geometry. *Appl Phys Lett* **115**, 051101 (2019).
83. Wu HJ, Zhou ZY, Gao W, Shi BS, Zhu ZH. Dynamic tomography of the spin-orbit coupling in nonlinear optics. *Phys Rev A* **99**, 023830 (2019).
84. Bouchard F, Larocque H, Yao AM, Travis C, De Leon I et al. Polarization shaping for control of nonlinear prop-agation. *Phys Rev Lett* **117**, 233903 (2016).
85. Yang C, Zhou ZY, Li Y, Li YH, Liu SL et al. Nonlinear frequency conversion and manipulation of vector beams in a Sagnac loop. *Opt Lett* **44**, 219–222 (2019).
86. Ren ZC, Lou YC, Cheng ZM, Fan L, Ding JP et al. Optical frequency conversion of light with maintaining polarization and orbital angular momentum. *Opt Lett* **46**, 2300–2303 (2021).
87. Samim M, Krouglov S, Barzda V. Nonlinear Stokes-Mueller polarimetry. *Phys Rev A* **93**, 013847 (2016).
88. Ribeiro PHS, Caetano DP, Almeida MP, Huguenin JA, dos Santos BC et al. Observation of image transfer and phase conjugation in stimulated down-conversion. *Phys Rev Lett* **87**, 133602 (2001).
89. de Oliveira AG, Arruda MFZ, Soares WC, Walborn SP, Khoury AZ et al. Phase conju-gation and mode conversion in stimulated parametric down-conversion With orbital angular momentum: a ge-ometrical interpretation. *Braz J Phys* **49**, 10–16 (2019).
90. de Oliveira AG, Arruda MFZ, Soares WC, Walborn SP, Gomes RM et al. Real-time phase conjugation of vector vortex beams. *ACS Photonics* **7**, 249–255 (2020).
91. de Oliveira AG, da Silva NR, de Araújo RM, Ribeiro PHS, Walborn SP. Quantum optical description of phase conjugation of vector vortex beams in stimulated parametric down-conversion. *Phys Rev Appl* **14**, 024048 (2020).
92. da Silva NR, de Oliveira AG, Arruda MFZ, de Araújo RM, Soares WC et al. Stimulated parametric down-conversion With vector vortex beams. *Phys Rev Appl* **15**, 024039 (2021).
93. Brenier A. Investigation of the sum of orbital angular momentum generated by conical diffraction. *J Opt* **22**, 045603 (2020).
94. Yu HH, Zhang HJ, Wang ZP, Wang JY, Pan ZB et al. Experimental observation of optical vortex in self-frequency-doubling generation. *Appl Phys Lett* **99**, 241102 (2011).
95. Zolotovskaya SA, Abdolvand A, Kalkandjiev TK, Rafailov EU. Second-harmonic conical refraction: observation of free and forced harmonic Waves. *Appl Phys B* **103**, 9–12 (2011).
96. Peet V, Shchemelyov S. Frequency doubling with laser beams transformed by conical refraction in a biaxial crystal. *J Opt* **13**, 055205 (2011).
97. Tang YT, Li KF, Zhang XC, Deng JH, Li GX et al. Harmonic spin-orbit angular momentum cascade in nonlinear optical crystals. *Nat Photonics* **14**, 658–662 (2020).
98. Forbes A. Structured light from lasers. *Laser Photonics Rev* **13**, 1900140 (2019).
99. Forbes A. Controlling light's helicity at the source: orbital angular momentum states from lasers. *Philos Trans A Math Phys Eng Sci* **375**, 20150436 (2017).
100. Omatsu T, Miyamoto K, Lee AJ. Wavelength-versatile optical vortex lasers. *J Opt* **19**, 123002 (2017).
101. Naidoo D, Roux FS, Dudley A, Litvin I, Piccirillo B et al. Controlled generation of higher-order Poincaré sphere beams from a laser. *Nat Photonics* **10**, 327–332 (2016).
102. Wei DZ, Cheng Y, Ni R, Zhang Y, Hu XP et al. Generating controllable Laguerre-Gaussian laser modes through intracavity spin-orbital angular momentum conversion of light. *Phys Rev Appl* **11**, 014038 (2019).
103. Yusufu T, Niu SJ, Tuersun P, Tulake Y, Miyamoto K et al. Tunable 3 μm optical vortex parametric oscillator. *Jpn J Appl Phys* **57**, 122701 (2018).
104. Zhou N, Liu J, Wang J. Reconfigurable and tunable twisted light laser. *Sci Rep* **8**, 11394 (2018).
105. Sroor H, Lisa N, Naidoo D, Litvin I, Forbes A. Cylindrical vector beams through amplifiers. *Proc SPIE* **10511**, 105111M (2018).
106. Ahmed MA, Beirow F, Loescher A, Dietrich T, Bashir D et al. High-power thin-disk lasers emitting beams with axially-symmetric polarizations. *Nanophotonics* **11**, 835–846 (2022).
107. Zhong HZ, Liang CC, Dai SY, Huang JF, Hu SS et al. Polarization-insensitive, high-gain parametric amplification of radially polarized femtosecond pulses. *Optica* **8**, 62–69 (2021).
108. Jung Y, Kang QY, Sidharthan R, Ho D, Yoo S et al. Optical orbital angular momentum amplifier based on an air-hole erbium-doped fiber. *J Lightwave Technol* **35**, 430–436 (2017).
109. Zhu S, Pidishety S, Feng YT, Hong S, Demas J et al. Multimode-pumped Raman amplification of a higher order mode in a large mode area fiber. *Opt Express* **26**, 23295–23304 (2018).
110. Bell T, Kgomo M, Ngcobo S. Digital laser for on-demand intracavity selective excitation of second harmonic higher-order modes. *Opt Express* **28**, 16907–16923 (2020).
111. Sroor H, Huang YW, Sephton B, Naidoo D, Vallés A et al. High-purity orbital angular momentum states from a visible metasurface laser. *Nat Photonics* **14**, 498–503 (2020).
112. Rao AS, Miike T, Miyamoto K, Omatsu T. Optical vortex lattice mode generation from a diode-pumped Pr^{3+}: $LiYF_4$ laser. *J Opt* **23**, 075502 (2021).

113. Rao AS, Miamoto K, Omatsu T. Ultraviolet intracavity frequency-doubled Pr^{3+}: $LiYF_4$ orbital Poincaré laser. *Opt Express* **28**, 37397–37405 (2020).
114. Vaupel M, Maître A, Fabre C. Observation of pattern formation in optical parametric oscillators. *Phys Rev Lett* **83**, 5278–5281 (1999).
115. Marte M, Ritsch H, Petsas KI, Gatti A, Lugiato LA et al. Spatial patterns in optical parametric oscillators with spherical mirrors: classical and quantum effects. *Opt Express* **3**, 71–80 (1998).
116. Ducci S, Treps N, Maître A, Fabre C. Pattern formation in optical parametric oscillators. *Phys Rev A* **64**, 023803 (2001).
117. Lassen M, Delaubert V, Janousek J, Wagner K, Bachor HA et al. Tools for multimode quantum information: modulation, detection, and spatial quantum correlations. *Phys Rev Lett* **98**, 083602 (2007).
118. Martinelli M, Huguenin JAO, Nussenzveig P, Khoury AZ. Orbital angular momentum exchange in an optical parametric oscillator. *Phys Rev A* **70**, 013812 (2004).
119. Barros RF, Alves GB, Tasca DS, Souza CER, Khoury AZ. Fine-tuning of orbital angular momentum in an optical parametric oscillator. *J Phys B At Mol Opt Phys* **52**, 244002 (2019).
120. Qi T, Wang DM, Gao W. Sum-frequency generation of ring-airy beams. *Appl Phys B* **128**, 67 (2022).
121. Dolev I, Ellenbogen T, Arie A. Switching the acceleration direction of airy beams by a nonlinear optical process. *Opt Lett* **35**, 1581–1583 (2010).
122. Ni R, Niu YF, Du L, Hu XP, Zhang Y et al. Topological charge transfer in frequency doubling of fractional orbital angular momentum state. *Appl Phys Lett* **109**, 151103 (2016).
123. Dmitriev VG, Gurzadyan GG, Nikogosyan DN. *Handbook of Nonlinear Optical Crystals* 2nd ed (Springer, Berlin, 1997).
124. Berger V. Nonlinear photonic crystals. *Phys Rev Lett* **81**, 4136–4139 (1998).
125. Saltiel S, Kivshar YS. Phase matching in nonlinear $\chi^{(2)}$ photonic crystals. *Opt Lett* **25**, 1204–1206 (2000).
126. Arie A, Voloch N. Periodic, quasi-periodic, and random quadratic nonlinear photonic crystals. *Laser Photonics Rev* **4**, 355–373 (2010).
127. Zhang Y, Wen JM, Zhu SN, Xiao M. Nonlinear Talbot effect. *Phys Rev Lett* **104**, 183901 (2010).
128. Shapira A, Juwiler I, Arie A. Nonlinear computer-generated holograms. *Opt Letters* **36**, 3015–3017 (2011).
129. Shapira A, Shiloh R, Juwiler I, Arie A. Two-dimensional nonlinear beam shaping. *Opt Lett* **37**, 2136–2138 (2012).
130. Bloch NV, Shemer K, Shapira A, Shiloh R, Juwiler I et al. Twisting light by nonlinear photonic crystals. *Phys Rev Lett* **108**, 233902 (2012).
131. Shiloh R, Arie A. Spectral and temporal holograms with nonlinear optics. *Opt Lett* **37**, 3591–3593 (2012).
132. Leshem A, Shiloh R, Arie A. Experimental realization of spectral shaping using nonlinear optical holograms. *Opt Lett* **39**, 5370–5373 (2014).
133. Chen PC, Wang CW, Wei DZ, Hu YL, Xu XY et al. Quasi-phase-matching-division multiplexing holography in a three-dimensional nonlinear photonic crystal. *Light Sci Appl* **10**, 146 (2021).
134. Lou YC, Cheng ZM, Liu ZH, Yang YX, Ren ZC et al. Third-harmonic generation of spatially structured light in a quasi-periodically poled crystal. *Optica* **9**, 183–186 (2022).
135. Chen Y, Ni R, Wu YD, Du L, Hu XP et al. Phase-matching controlled orbital angular momentum conversion in periodically poled crystals. *Phys Rev Lett* **125**, 143901 (2020).
136. Wei DZ, Wang CW, Wang HJ, Hu XP, Wei D et al. Experimental demonstration of a three-dimensional lithium niobate nonlinear photonic crystal. *Nat Photonics* **12**, 596–600 (2018).
137. Keren-Zur S, Ellenbogen T. A new dimension for nonlinear photonic crystals. *Nat Photonics* **12**, 575–577 (2018).
138. Wei DZ, Wang CW, Xu XY, Wang HJ, Hu YL et al. Efficient nonlinear beam shaping in three-dimensional lithium niobate nonlinear photonic crystals. *Nat Communications* **10**, 4193 (2019).
139. Zhang Y, Sheng Y, Zhu SN, Xiao M, Krolikowski W. Nonlinear photonic crystals: from 2D to 3D. *Optica* **8**, 372–381 (2021).
140. Lee HJ, Kim H, Cha M, Moon HS. Simultaneous type-0 and type-II spontaneous parametric downconversions in a single periodically poled $KTiOPO_4$ crystal. *Appl Phys B* **108**, 585–589 (2012).
141. Zhang WG, Yu HW, Wu HP, Halasyamani PS. Phase-matching in nonlinear optical compounds: a materials perspective. *Chem Mater* **29**, 2655–2668 (2017).
142. Jáuregui R, Torres JP. On the use of structured light in nonlinear optics studies of the symmetry group of a crystal. *Sci Repo* **6**, 20906 (2016).
143. Chen SM, Li KF, Deng JH, Li GX, Zhang S. High-order nonlinear spin-orbit interaction on plasmonic metasurfaces. *Nano Lett* **20**, 8549–8555 (2020).
144. Schlickriede C, Kruk SS, Wang L, Sain B, Kivshar Y et al. Nonlinear imaging with all-dielectric metasurfaces. *Nano Lett* **20**, 4370–4376 (2020).
145. Rahmani M, Leo G, Brener I, Zayats AV, Maier SA et al. Nonlinear frequency conversion in optical nanoantennas and metasurfaces: materials evolution and fabrication. *Opto-Electron Adv* **1**, 180021 (2018).
146. Zhang YB, Liu H, Cheng H, Tian JG, Chen SQ. Multidimensional manipulation of wave fields based on artificial microstructures. *Opto-Electron Adv* **3**, 200002 (2020).
147. Pertsch T, Kivshar Y. Nonlinear optics with resonant metasurfaces. *MRS Bull* **45**, 210–220 (2020).
148. Grinblat G. Nonlinear dielectric nanoantennas and metasurfaces: frequency conversion and wavefront control. *ACS Photonics* **8**, 3406–3432 (2021).
149. Wang L, Kruk S, Koshelev K, Kravchenko I, Luther-Davies B et al. Nonlinear wavefront control with all-dielectric metasurfaces. *Nano Lett* **18**, 3978–3984 (2018).
150. Li GX, Chen SM, Pholchai N, Reineke B, Wong PWH et al. Continuous control of the nonlinearity phase for harmonic generations. *Nat Mater* **14**, 607–612 (2015).
151. Gao YS, Fan YB, Wang YJ, Yang WH, Song QH et al. Nonlinear holographic all-dielectric metasurfaces. *Nano Lett* **18**, 8054–8061 (2018).
152. Li GX, Wu L, Li KF, Chen SM, Schlickriede C et al. Nonlinear metasurface for simultaneous control of spin and orbital angular momentum in second harmonic generation. *Nano Lett* **17**, 7974–7979 (2017).
153. Walter F, Li GX, Meier C, Zhang S, Zentgraf T. Ultrathin nonlinear metasurface for optical image encoding. *Nano Lett* **17**, 3171–3175 (2017).
154. Chen SM, Reineke B, Li GX, Zentgraf T, Zhang S. Strong nonlinear optical activity induced by lattice surface modes on Plasmonic metasurface. *Nano Lett* **19**, 6278–6283 (2019).

155. Yariv A. Four wave nonlinear optical mixing as real time holography. *Opt Commun* **25**, 23–25 (1978).
156. Liu HG, Li J, Fang XL, Zhao XH, Zheng YL et al. Dynamic computer-generated nonlinear-optical holograms. *Phys Rev A* **96**, 023801 (2017).
157. Qiu XD, Li FS, Liu HG, Chen XF, Chen LX. Optical vortex copier and regenerator in the Fourier domain. *Photonics Res* **6**, 641–646 (2018).
158. Liu HG, Zhao XH, Li H, Zheng YL, Chen XF. Dynamic computer-generated nonlinear optical holograms in a non-collinear second-harmonic generation Process. *Opt Lett* **43**, 3236–3239 (2018).
159. Liu S, Mazur LM, Krolikowski W, Sheng Y. Nonlinear volume holography in 3D nonlinear photonic crystals. *Laser Photonics Rev* **14**, 2000224 (2020).
160. Hong XH, Yang B, Zhang C, Qin YQ, Zhu YY. Nonlinear volume holography for wave-front engineering. *Phys Rev Lett* **113**, 163902 (2014).
161. Trajtenebrg-Mills S, Arie A. Shaping light beams in nonlinear processes using structured light and patterned crystals. *Opt Mater Express* **7**, 2928–2942 (2017).
162. Shapira A, Naor L, Arie A. Nonlinear optical holograms for spatial and spectral shaping of light waves. *Sci Bull* **60**, 1403–1415 (2015).
163. Liu HG, Chen XF. The manipulation of second-order nonlinear harmonic wave by structured material and structured light. *J Nonlinear Opt Phys Mater* **27**, 1850047 (2018).
164. Tabosa JWR, Petrov DV. Optical pumping of orbital angular momentum of light in cold cesium atoms. *Phys Rev Lett* **83**, 4967–4970 (1999).
165. Barreiro S, Tabosa JWR, Torres JP, Deyanova Y, Torner L. Four-wave mixing of light beams with engineered orbital angular momentum in cold cesium atoms. *Opt Lett* **29**, 1515–1517 (2004).
166. Prajapati N, Super N, Lanning NR, Dowling JP, Novikova I. Optical angular momentum manipulations in a four-wave mixing process. *Opt Lett* **44**, 739–742 (2019).
167. Offer RF, Stulga D, Riis E, Franke-Arnold S, Arnold AS. Spiral bandwidth of four-wave mixing in Rb vapour. *Commun Phys* **1**, 84 (2018).
168. Danaci O, Rios C, Glasser RT. All-optical mode conversion via spatially multimode four-wave mixing. *New J Phys* **18**, 073032 (2016).
169. Knutson EM, Swaim JD, Wyllie S, Glasser RT. Optimal mode configuration for multiple phase-matched four-wave-mixing processes. *Phys Rev A* **98**, 013828 (2018).
170. Offer RF, Daffurn A, Riis E, Griffin PF, Arnold AS et al. Gouy phase-matched angular and radial mode conversion in four-wave mixing. *Phys Rev A* **103**, L021502 (2021).
171. Swaim JD, Knutson EM, Danaci O, Glasser RT. Multimode four-wave mixing with a spatially structured pump. *Opt Lett* **43**, 2716–2719 (2018).
172. Hasan SB, Lederer F, Rockstuhl C. Nonlinear plasmonic antennas. *Mater Today* **17**, 478–485 (2014).
173. Kauranen M, Zayats AV. Nonlinear plasmonics. *Nat Photonics* **6**, 737–748 (2012).
174. Grinblat G, Li Y, Nielsen MP, Oulton RF, Maier SA. Degenerate four-wave mixing in a multiresonant germanium nanodisk. *ACS Photonics* **4**, 2144–2149 (2017).
175. Corkum PB. Plasma perspective on strong field multiphoton ionization. *Phys Rev Lett* **71**, 1994–1997 (1993).
176. Fleischer A, Kfir O, Diskin T, Sidorenko P, Cohen O. Spin angular momentum and tunable polarization in high-harmonic generation. *Nat Photonics* **8**, 543–549 (2014).
177. Huang PC, Hernández-García C, Huang JT, Huang PY, Lu CH et al. Polarization control of isolated high-harmonic pulses. *Nat Photonics* **12**, 349–354 (2018).
178. Gariepy G, Leach J, Kim KT, Hammond TJ, Frumker E et al. Creating high-harmonic beams with controlled orbital angular momentum. *Phys Rev Lett* **113**, 153901 (2014).
179. Gauthier D, Ribič PR, Adhikary G, Camper A, Chappuis C et al. Tunable orbital angular momentum in high-harmonic generation. *Nat Commun* **8**, 14971 (2017).
180. Géneaux R, Chappuis C, Auguste T, Beaulieu S, Gorman TT et al. Radial index of Laguerre-Gaussian modes in high-order-harmonic generation. *Phys Rev A* **95**, 051801 (2017).
181. Chappuis C, Bresteau D, Auguste T, Gobert O, Ruchon T. High-order harmonic generation in an active grating. *Phys Rev A* **99**, 033806 (2019).
182. Hareli L, Lobachinsky L, Shoulga G, Eliezer Y, Michaeli L et al. On-the-fly control of high-harmonic generation using a structured pump beam. *Phys Rev Lett* **120**, 183902 (2018).
183. Panagiotopoulos P, Papazoglou DG, Couairon A, Tzortzakis S. Sharply autofocused ring-Airy beams transforming into non-linear intense light bullets. *Nat Commun* **4**, 2622 (2013).
184. Dorney KM, Rego L, Brooks NJ, Román JS, Liao CT et al. Controlling the polarization and vortex charge of attosecond high-harmonic beams via simultaneous spin-orbit momentum conservation. *Nat Photonics* **13**, 123–130 (2019).
185. Kong F, Zhang C, Larocque H, Bouchard F, Li Z et al. Spin-constrained orbital-angular-momentum control in high-harmonic generation. *Phys Rev Res* **1**, 032008 (2019).
186. Géneaux R, Camper A, Auguste T, Gobert O, Caillat J et al. Synthesis and characterization of attosecond light vortices in the extreme ultraviolet. *Nat Commun* **7**, 12583 (2016).
187. Rego L, Dorney KM, Brooks NJ, Nguyen QL, Liao CT et al. Generation of extreme-ultraviolet beams with time-varying orbital angular momentum. *Science* **364**, eaaw9486 (2019).
188. Barreiro S, Tabosa JWR. Generation of light carrying orbital angular momentum via induced coherence grating in cold atoms. *Phys Rev Lett* **90**, 133001 (2003).
189. Pugatch R, Shuker M, Firstenberg O, Ron A, Davidson N. Topological stability of stored optical vortices. *Phys Rev Lett* **98**, 203601 (2007).
190. Moretti D, Felinto D, Tabosa JWR. Collapses and revivals of stored orbital angular momentum of light in a cold-atom ensemble. *Phys Rev A* **79**, 023825 (2009).
191. de Almeida AJF, Barreiro S, Martins WS, de OliVeira RA, Felinto D et al. Storage of orbital angular momenta of light via coherent population oscillation. *Opt Lett* **40**, 2545–2548 (2015).
192. de Oliveira RA, Borba GC, Martins WS, Barreiro S, Felinto D et al. Nonlinear optical memory for manipulation of orbital angular momentum of light. *Opt Lett* **40**, 4939–4942 (2015).
193. Veissier L, Nicolas A, Giner L, Maxein D, Sheremet AS et al. Reversible optical memory for twisted photons. *Opt Lett* **38**, 712–714 (2013).
194. Sukhorukov AP, Yangirova VV. Spatio-temporal vortices: properties, generation and recording. *Proc SPIE* **5949**, 594906 (2005).
195. Gui G, Brooks NJ, Kapteyn HC, Murnane MM, Liao CT.

Second-harmonic generation and the conservation of spatiotemporal orbital angular momentum of light. *Nat Photonics* **15**, 608–613 (2021).
196. Hancock SW, Zahedpour S, Milchberg HM. Second-harmonic generation of spatiotemporal optical vortices and conservation of orbital angular momentum. *Optica* **8**, 594–597 (2021).
197. Desyatnikov AS, Kivshar YS, Torner L. Optical vortices and vortex solitons. *Prog Opt* **47**, 291–391 (2005).
198. Kivshar YS, Pelinovsky DE. Self-focusing and transverse instabilities of solitary waves. *Phys Rep* **331**, 117–195 (2000).
199. Reyna AS, de Araújo CB. Spatial phase modulation due to quintic and septic nonlinearities in metal colloids. *Opt Express* **22**, 22456–22469 (2014).
200. Reyna AS, de Araújo CB. Nonlinearity management of photonic composites and observation of spatial-modulation instability due to quintic nonlinearity. *Phys Rev A* **89**, 063803 (2014).
201. Reyna AS, Jorge KC, de Araújo CB. Two-dimensional solitons in a quintic-septimal medium. *Phys Rev A* **90**, 063835 (2014).
202. Reyna AS, Malomed BA, de Araújo CB. Stability conditions for one-dimensional optical solitons in cubic-quintic-septimal media. *Phys Rev A* **92**, 033810 (2015).
203. Reyna AS, Bergmann E, Brevet PF, de Araújo CB. Nonlinear polarization instability in cubic-quintic plasmonic nanocomposites. *Opt Express* **25**, 21049–21067 (2017).
204. Reyna AS, Boudebs G, Malomed BA, de Araújo CB. Robust self-trapping of vortex beams in a saturable optical medium. *Phys Rev A* **93**, 013840 (2016).
205. Kivshar Y. Bending light at will. *Nat Phys* **2**, 729–730 (2006).
206. Kivshar YS, Stegeman GI. Spatial optical solitons. *Opt Photonics News* **13**, 59–63 (2002).
207. Chen ZG, Segev M, Christodoulides DN. Optical spatial solitons: historical overview and recent advances. *Rep Prog Phys* **75**, 086401 (2012).
208. Reyna AS, de Araújo CB. High-order optical nonlinearities in plasmonic nanocomposites—a review. *Adv Opt Photonics* **9**, 720–774 (2017).
209. Kong FQ, Zhang CM, Bouchard F, Li ZY, Brown GG et al. Controlling the orbital angular momentum of high harmonic vortices. *Nat Commun* **8**, 14970 (2017).
210. Couteau C. Spontaneous parametric down-conversion. *Contemp Phys* **59**, 291–304 (2018).
211. Romero J, Giovannini D, McLaren MG, Galvez EJ, Forbes A et al. Orbital angular momentum correlations with a phase-flipped Gaussian mode pump beam. *J Opt* **14**, 085401 (2012).
212. Walborn SP, de Oliveira AN, Pádua S, Monken CH. Multimode hong-ou-mandel interference. *Phys Rev Lett* **90**, 143601 (2003).
213. Yao AM. Angular momentum decomposition of entangled photons with an arbitrary pump. *New J Phys* **13**, 053048 (2011).
214. Vicuña-Hernández V, Santiago JT, Jerónimo-Moreno Y, Ramírez-Alarcón R, Cruz-Ramírez H et al. Double transverse wave-vector correlations in photon pairs generated by spontaneous parametric down-conversion pumped by Bessel-Gauss beams. *Phys Rev A* **94**, 063863 (2016).
215. Torres JP, Deyanova Y, Torner L, Molina-Terriza G. Preparation of engineered two-photon entangled states for multidimensional quantum information. *Phys Rev A* **67**, 052313 (2003).
216. Khoury AZ, Ribeiro PHS, Dechoum K. Transfer of angular spectrum in parametric down-conversion with structured light. *Phys Rev A* **102**, 033708 (2020).
217. Hu XM, Zhang C, Guo Y, Wang FX, Xing WB et al. Pathways for entanglement-based quantum communication in the face of high noise. *Phys Rev Lett* **127**, 110505 (2021).
218. Hu XM, Xing WB, Liu BH, Huang YF, Li CF et al. Efficient generation of high-dimensional entanglement through multipath down-conversion. *Phys Rev Lett* **125**, 090503 (2020).
219. Baghdasaryan B, Fritzsche S. Enhanced entanglement from Ince-Gaussian pump beams in spontaneous parametric down-conversion. *Phys. Rev. A* **102**, 052412 (2020).
220. Liu SL, Zhang YW, Yang C, Liu SK, Ge Z et al. Increasing two-photon entangled dimensions by shaping input-beam profiles. *Phys Rev A* **101**, 052324 (2020).
221. Chen YY, Zhang WH, Zhang DK, Qiu XD, Chen LX. Coherent genera-tion of the complete high-dimensional bell basis by adaptive pump modulation. *Phys Rev Appl* **14**, 054069 (2020).
222. van der Meer R, Renema JJ, Brecht B, Silberhorn C, Pinkse PWH. Optimizing spontaneous parametric down-conversion sources for boson sampling. *Phys Rev A* **101**, 063821 (2020).
223. Bornman N, Buono WT, Lovemore M, Forbes A. Optimal pump shaping for entanglement control in any countable basis. *Adv Quantum Technol* **4**, 2100066 (2021).
224. Chang DE, Vuletić V, Lukin MD. Quantum nonlinear optics — photon by photon. *Nat Photonics* **8**, 685–694 (2014).
225. Guerreiro T, Martin A, Sanguinetti B, Pelc JS, Langrock C et al. Nonlinear interaction between Single Photons. *Phys Rev Lett* **113**, 173601 (2014).
226. Molotkov SN. Quantum teleportation of a single-photon wave packet. *Phys Lett A* **245**, 339–344 (1998).
227. Molotkov SN. Experimental scheme for quantum teleportation of a one-photon packet. *J Exp Theor Phys Lett* **68**, 263–270 (1998).
228. Walborn SP, Monken CH, Pádua S, Ribeiro PHS. Spatial correlations in parametric down-conversion. *Phys Rep* **495**, 87–139 (2010).
229. Humble TS. Spectral and spread-spectral teleportation. *Phys Rev A* **81**, 062339 (2010).
230. Kim YH, Kulik SP, Shih Y. Quantum teleportation of a polarization state with a complete bell state measurement. *Phys Rev Lett* **86**, 1370–1373 (2001).
231. Sangouard N, Sanguinetti B, Curtz N, Gisin N, Thew R et al. Faithful entanglement swapping based on sum-frequency generation. *Phys Rev Lett* **106**, 120403 (2011).
232. Gisin N, Pironio S, Sangouard N. Proposal for implementing device-independent quantum key distribution based on a heralded qubit amplifier. *Phys Rev Lett* **105**, 070501 (2010).
233. Minář J, de Riedmatten H, Sangouard N. Quantum repeaters based on heralded qubit amplifiers. *Phys Rev A* **85**, 032313 (2012).
234. Sephton B, Vallés A, Nape I, Cox MA, Steinlechner F et al. High-dimensional spatial teleportation enabled by nonlinear optics. arXiv: 2111.13624, 2021.

Competing interests

The authors declare no competing financial interests.